CHEMICAL ENGINEERING TRANSACTIONS
VOL. 62, 2017
A publication of AIDIC
The Italian Association of Chemical Engineering
Online at www.aidic.it/cet
Guest Editors: Fei Song, Haibo Wang, Fang He

ISBN 978-88-95608- 60-0; **ISSN** 2283-9216
DOI: 10.3303/CET1762170

Study on Vertical Bearing Capacity Change of Single Pile under Dry Condition and Submerged Condition in Loess Collapse Region

Binwei Zhang*[ab], Songhong Yan[c]

[ac]School of Civil Engineering, Lanzhou Jiaotong University,Lanzhou 730070,China
[b]School of Civil Engineering, Longdong University,Qingyang 745000,China
zbwei3000@163.com

In order to study the change of vertical bearing characteristics of single pile under dry state and flooded state in loessial collapsible area, this study conducted a flooding test on site. The experiment reveals the law of the effect of ground immersion on the bearing capacity of bridge pile foundation in the loess region, and analyzes the characteristics of settlement variation during the flooding of pile and surrounding soil. Immersion test results show that the pile and pile around the average settlement of soil is 0.15mm and 1.4mm. After the pile side of the soil is flooded, the pile and its surrounding soil have varying degrees of settlement deformation. The settlement of the soil around the pile is caused by the weak collapsibility of the loess. The settlement deformation of the pile is caused by the negative friction caused by the collapsible loess on the pile. Therefore, the ultimate bearing capacity of the soaking is obviously different, the former is greater than 9600kN and the latter is 8000kN. Carrying capacity test has been carried out several times, its ultimate bearing capacity is consistent.

1. Introduction

The pile is a cylindrical member that can be inserted into the soil. Based on weaker formations or water, it can transfer superstructure loads to harder, less compressible soil or rock formations (Xiong et al., 2016). From a historical perspective, pile is not only an ancient foundation, but also the most widely used foundation of buildings. Pile is a deep foundation (Smalley et al., 2016). Pile foundation with high bearing capacity, great reliability. In addition, its scope of application is very wide. Therefore, the pile is widely used in the bridge foundation. Loess is a facies sedimentary facies of the Quaternary (Maher, 2016). It has macropores, vertical joints and tubular channels. In terms of natural water content, loess is more intense and it can maintain very high vertical slopes (Smalley, et al., 2016). However, when the loess encounters water, the soil particles are disintegrated Loess is collapsible under some conditions. Therefore, loess is divided into non-collapsible loess and collapsible loess (Zhuang, et al., 2016).

Loess collapses with water and it produces negative friction at the pile circumference, which affects the bearing capacity of the pile (Lehmkuhl et al., 2016). The pile bearing capacity test was carried out before and after the pile foundation in the loess area was flooded (Valaee et al., 2016). In addition, the changing traits of the bearing capacity of the pile before and after immersion in the loess were analyzed, and the pile of lateral resistance variation was also analyzed (Sun et al., 2016). Based on the analysis of the settlement and deformation of the pile itself and the soil around the pile during the immersion period, the bearing capacity of the pile before and after immersion is evaluated based on the design data and theoretical analysis of the bridge (Bjelajac et al., 2016).

Please cite this article as: Binwei Zhang, Songhong Yan, 2017, Study on vertical bearing capacity change of single pile under dry condition and submerged condition in loess collapse region, Chemical Engineering Transactions, 62, 1015-1020 DOI:10.3303/CET1762170

2. Experimental design

2.1 Test element layout

The test element is set to collect the relevant data of the deformation and internal force variation and distribution after the test pile is loaded. Therefore, the rationality of its embedded will be directly related to the authenticity of data processing results. In this test, the test elements are steel bars, concrete strain gauges and dial gauges (Jin et al., 2016). When installing the embedded parts, we should pay attention to the following two points. First, the main reinforcement bars and test tendons are welded together in series. At the same time, the welding temperature should not be too high (Miyazaki et al., 2016). In the process of processing, soaking wet towel cooling measures are used. Second, the concrete strain gauge should be fixed around the force of steel, so as not to slip during the concrete pouring loose (Liu et al., 2016).

The dial indicator is laid for measuring the settlement of the pile at each level of loading. In the field test, the dial indicator is mounted in two orthogonal diameter directions of the pile with a measuring range of 50 mm. The distance from pile top to settlement measuring plane is 80cm, and the bracket is installed in this plane. In addition, the dial indicator magnetic bracket and support stand and reference beam is fixed (Licht et al., 2016). Under certain circumstances, temperature and other factors will have an impact on it, so insulation measures are taken. When installing the dial indicator, we should pay attention to the following points. First, the magnetic holder of the dial indicator should be firmly fixed on the reference beam (Zhang et al., 2016). Second, the dial indicator rod and bracket should be in close contact with the indicator rod upright. Finally, the initial reading of the dial indicator should be adjusted to zero before starting to load (Wang et al., 2016).

2.2 Anti-force beam design

In the determination of the length of the reaction beam, its length needs to meet the requirements of various pile spacing in the test. Therefore, through theoretical calculations and multi-argument, the length of the beam was determined to be 11.2 meters and the design tonnage was 800 tons. The design of the anti-force beam is more complex because of its large span and the large flexibility which are the common features of the steel beam. Therefore, the stiffness is the main factor in the design of the reaction beam. In a sense, the strength requirements are easily met, but the stiffness requirements are hard to meet. In addition, according to the force characteristics of the reaction beam, the design of the variable section steel beam is adopted. Although this approach has increased the difficulty of processing, it greatly reduces the amount of material. It also reduces self-weight while reducing deflection under design loads and meets design requirements. Studies have shown that when the pile top is loaded to 8000kN, the deflection of the reaction girder is less than 7mm. This figure is basically in line with expectations.

In order to facilitate the connection between anchor bar and anti-force girder, bolts are used to fix the anchor plate on the reaction girder. Practice has proved that this anchor plate can freely move the anchor system. Therefore, it has the advantages of saving materials and improving the overall stability of the structure. The rational design of the reaction beam is an important guarantee for the successful loading of the entire test. In design, the following principles should be followed. Firstly, the strength of the reaction beam should be secured, and its safety must also be determined. Secondly, the stiffness of the reaction beam should be protected. Under the reaction force of 10000kN, it will not be destroyed. In the design reaction force, excessive deformation will not happen. Moreover, the overall and partial stability of the reaction beam should be protected so that it will not be destabilized under high stress conditions. Finally, the overall connection of the reaction girder and the reliability of the partial pressure shall be ensured so as to minimize the loss of the jack stroke, so as to meet the requirements of local pressure bearing.

2.3 Test loading and testing

The test includes the settlement of pile top, the stress and strain of pile cross-section and the stress of reinforcement. Pile top settlement test is to measure the pile top settlement deformation under each load. Two iron and steel as the benchmark in the test beam, magnetic table mounted on the fixed dial indicator. In addition, there is a camera lens on each dial indicator. It uses a remote reading system that captures the dial indicator directly from the display, so as to read the pile top displacement test system. There are four dial indicators on the top of the test pile. The top displacement of the anchor can be monitored by a precision level.

Stress and strain of pile section are measured by reinforcing bars, concrete strain gauges and pressure boxes. Reading requirements include the following points. The initial reading of each component is read before the test is loaded. Later, when the load of each level reaches 30 minutes, its value needs to be read. When the top of the pile settles, its value needs to be read. In the unloading process, when the load reaches 30 minutes each level, its value needs to be read. After uninstallation, its value needs to be read every 4 hours.

3. Analysis of load test results

3.1 Bearing capacity analysis of pile after soaking

The negative friction on pile side is caused by the settlement deformation of pile side soil is greater than the pile settlement. Therefore, on the basis of the water immersion around the pile, this study studied the variation of negative friction resistance. Water immersion lasted 48 days, the amount of water soaking up to 6,000 cubic meters, after immersion soil around the pile settlement average 1.4cm. The results show that the loess in the experimental pile area is weakly collapsible loess or non-self-weight collapsible loess. During the settlement period of the pile soil, there is a great fluctuation due to the influence of climatic factors, and this phenomenon of rebound will occur. But eventually the amount of subsidence is created. In addition, the radial distribution of the settlement along the pile is also analyzed. The results show that under the influence of the boundary conditions, the settlement of the soil at the pile site and the edge of the foundation pit is small and the settlement in the middle part is relatively large.

At the same time, the distribution of settlement at the top of the pile settlement is analysed. The results show that the subsidence deformation of the pile during the immersion period is consistent with the soaking properties of the surrounding soil. In addition, under the influence of time, temperature and other factors, settlement deformation has rebounded. However, from the perspective of quantity, the settlement of pile top is much smaller than the settlement of soil around pile.

3.2 Bearing capacity of pile

Figure 1 is the No.1 test pile tip resistance distribution curve, Figure 2 is the No.1 test pile ΔS / S-Q distribution curve. It can be seen from Figure 1 and Figure 2 that when the load reaches 8000kN, the curve shows a significant inflection point. Therefore, the ultimate bearing capacity of pile No. 1 after soaking is 8000kN.

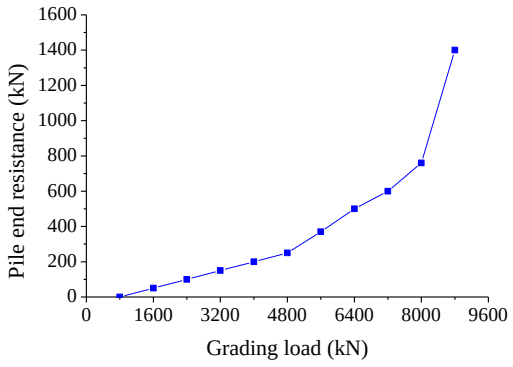

Figure 1: No.1 test pile tip resistance distribution curve

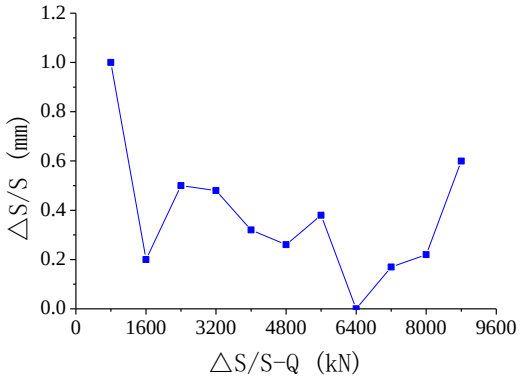

Figure 2: No.1 test pile ΔS / S-Q distribution curve

It can be seen from Figure 3 and Figure 4 that there is no obvious change in the settlement of the pile due to the influence of temperature. Therefore, the ultimate bearing capacity of pile No. 2 before soaking is more than 9600kN. This result shows that it is obviously larger than the design value (8000kN) of ultimate bearing capacity of pile in loess area.

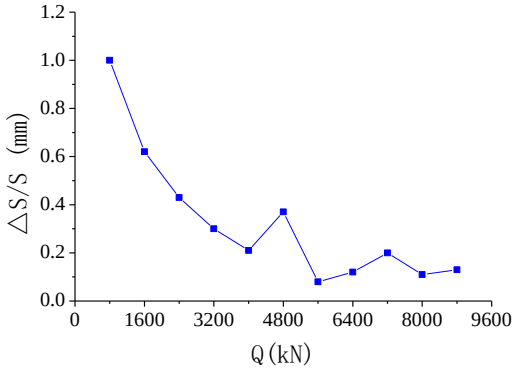

Figure 3: No.2 test pile △S/S-Q distribution curve

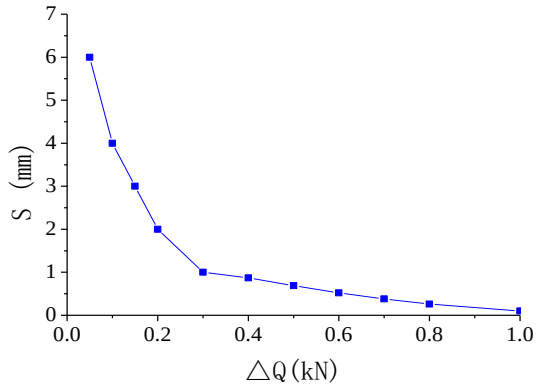

Figure 4: No.2 test pile △ Q / Q-S distribution curve

The ultimate bearing capacity of No. 2 pile before and after soaking has obvious difference, the former is much larger than the latter. Under the same load, the settlement of the pile before immersion is far less than the latter. This shows that the soaking of the soil around pile led to collapsibility of collapsible loess, and its shear strength decreased, which obviously affected the bearing capacity of pile. However, the test results also reflect that the negative frictional resistance of the pile side in this area is small, indicating that the loess collapsibility in the experimental area is small. Therefore, it belonged to weakly collapsible loess or non-gravity collapsible loess.

Table 1: Bearing capacity and settlement of pile before and after water immersion

	No.1 pile (soaking)	No.2 pile (soaking)	No.2 pile (Original soil)
Ultimate bearing capacity (kN)	8000	8000	9600
Settlement (mm)	5.30	5.97	6.04

3.3 Analysis of lateral resistance of pile

First, the side-resistance characteristics of pile before water immersion. The greater the axial force difference between piles and soil layers, the greater the slope of the axial force curve and the greater the lateral resistance between soil layers. When the load is small, the side resistance is smaller. As the loading level increases, the

resistance on the pile side gradually increases. When the load is 4800 kN, the soil layer in the partial area of the pile reaches the limit side frictional resistance value. When the load is 9600kN, the lateral resistance of most of the soil above 26m reaches the limit value. Pile side soil reaches the limit state side of the resistance value between 29.75-99.87kPa. The limit value of side resistance up to 177.12kPa.

Second, the side-resistance characteristics of pile after water immersion. When the load is small, the deformation of the pile is less, and the piles of some soil layers have negative friction. With the increase of load, the settlement of pile deformation also increases, and the corresponding negative friction decreases. When the loads of different soil layers increase by different values, most of the original negative-friction soil layers begin to provide positive frictional resistance. While some soil does not appear negative friction, its pile side resistance has reached the limit state. In addition, the geological survey shows that the material above 20m is loess and the material under 20m is red clay. At the same time, there is no negative friction appeared in the pile below 20m. The negative friction resistance of the first test pile varied from -5.20 to 69.44 kPa, the positive limit friction resistance varied from 29.39 to 86.71 kPa, and the maximum frictional resistance is 149.02 kPa. Changes in pile friction of before and after soaking are shown in Table 2.

Table 2: The maximum and minimum side friction of soil before and after immersion in water

Buried depth (m)	No.1 pile (kPa)	No.2 pile (kPa)
2	(56.70,1.41)	(39.26,13.11)
3	(76.00,2.32)	(41.39,2.09)
4	(81.92,17.77)	(54.25,5.97)
5	(77.29,12.96)	(43.66,10.51)
6	(63.89,0.69)	(37.06,9.02)

4. Conclusions

On the basis of the experimental study of on-site physical engineering, this study investigates the mechanical behavior of pile foundations in the loess area. The results of large-scale immersion tests show that the subsidence of pile-side soil makes the pile and its surrounding soil have different degrees of settlement due to the collapsibility of loess. Therefore, the average settlement of the soil around the pile and pile is 0.15mm and 1.4mm. The settlement deformation of the soil around the pile is caused by the collapsibility of the loess. The settlement deformation of the pile is due to the negative frictional resistance caused by the collapsibility of the pile.

Acknowledgments

This paper is a periodical research achievement of Gansu Natural Science Foundation of China(certificated number is 1506RJZM322)and Science Research fund of Gansu Provincial Education Department(certificated number is 2015A-151).The name of the above scientific research project is "Pile-Soil Interaction Theory and Experiment Research in Deep Loess of Longdong in Gansu Province of China ".

Reference

Bjelajac D., Mesaroš M., Schaetzl R.J., Pavic D., Micic T., Markovic R.S., 2016, Introducing the loess pyramid-an unusual landform in the thick loess deposits of vojvodina, serbia, Geographica Pannonica, 20(1), 1-7, DOI: 10.5937/geopan1601001b

Jin C., Liu Q., Hu P., Jiang Z., Li C., Han P., 2016, An integrated natural remanent magnetization acquisition model for the matuyama-brunhes reversal recorded by the Chinese loess, Geochemistry Geophysics Geosystems, 17(8), DOI: 10.1002/2016gc006407

Lehmkuhl F., Zens J., Krauß L., Schulte P., Kels H., 2016, Loess-paleosol sequences at the northern european loess belt in germany: distribution, geomorphology and stratigraphy, Quaternary Science Reviews, 153, 11-30, DOI: 10.1016/j.quascirev.2016.10.008

Licht A., Pullen A., Kapp P., Abell J., Giesler N., 2016, Eolian cannibalism: reworked loess and fluvial sediment as the main sources of the chinese loess plateau, Geological Society of America Bulletin, 128(5-6), B31375.1, DOI: 10.1130/b31375.1

Liu Z., Wei G., Wang X., Jin C., Liu Q., 2016, Quantifying paleoprecipitation of the luochuan and sanmenxia loess on the chinese loess plateau, Palaeogeography Palaeoclimatology Palaeoecology, 459, 121-130, DOI: 10.1016/j.palaeo.2016.06.034

Maher B.A., 2016, Palaeoclimatic records of the loess/palaeosol sequences of the chinese loess plateau, Quaternary Science Reviews, 154, 23-84, DOI: 10.1016/j.quascirev.2016.08.004

Miyazaki T., Kimura J., Katakuse M., 2016, Geochemical records from loess deposits in japan over the last 210 kyr: lithogenic source changes and paleoclimatic indications, Geochemistry Geophysics Geosystems, 17(7), DOI: 10.1002/2016gc006322

Smalley I., Kels H., Gaudenyi T., Jovanovic M., 2016, Loess encounters of three kinds: charles lyell talks about, reads about, and looks at loess, Geologos, 22(1), 71-77, DOI: 10.1515/logos-2016-0006

Smalley I.J., Bentley S.P., Markovic S.B., 2016, Loess and fragipans: development of polygonal-crack-network structures in fragipan horizons in loess ground, Quaternary International, 399, 228-233, DOI: 10.1016/j.quaint.2015.01.034

Sun Y., Liang L., Bloemendal J., Li Y., Wu F., Yao Z., 2016, High-resolution scanning xrf investigation of chinese loess and its implications for millennial-scale monsoon variability, Journal of Quaternary Science, 31(3), 191-202, DOI: 10.1002/jqs.2856

Valaee M., Ayoubi S., Khormali F., Lu S.G., Karimzadeh H.R., 2016, Using magnetic susceptibility to discriminate between soil moisture regimes in selected loess and loess-like soils in northern Iran, Journal of Applied Geophysics, 127, 23-30, DOI: 10.1016/j.jappgeo.2016.02.006

Wang C., Wang S., Fu B., Yang L., Li Z., 2017, Soil moisture variations with land use along the precipitation gradient in the north-south transect of the loess plateau, Land Degradation Development, 28, DOI: 10.1002/ldr.2604

Xiong L., Tang G., Strobl J., Zhu A., 2016, Paleotopographic controls on loess deposition in the loess plateau of china, Earth Surface Processes Landforms, 41(9), 1155-1168, DOI: 10.1002/esp.3883

Zhang L.T., Li Z.B., Wang S.S., 2016, Spatial scale effect on sediment dynamics in basin-wide floods within a typical agro-watershed: a case study in the hilly loess region of the Chinese loess plateau, Science of the Total Environment, 572, 476-486, DOI: 10.1016/j.scitotenv.2016.08.082

Zhuang Y., Bao W., French, C., 2016, Loess and early land use: geoarchaeological investigation at the early neolithic site of guobei, southern chinese loess plateau, Catena, 144, 151-162, DOI: 10.1016/j.catena.2016.05.005